Scaling and Modeling of Turbulent Suspension Flows

C. P. Chen
Department of Mechanical Engineering
University of Alabama in Huntsville
Huntsville, AL 35899

Introduction

The challenge of the study of gas-solid turbulent flows arises because of the complexity of physical interactions between the two phases. Research needs are also not universal for different situations. Depending on the particle loading ratios, particle sizes and particle-particle collision frequencies, the flow of gas-particle mixture law can be classified as dense flows or dilute flows. The characteristic dimensions of the distribution of particles in turbulent flows may determine whether the two-phase mixture can be regarded as a continuum or not [1,2]. In a dilute suspension flow in which particle motion is controlled by the aerodynamic forces on the particle, Crowe [3] has suggested a criterion for treating the particle cloud as a continuum. In this case, the Stokes number (St) which is defined $St = v_r t_* / \lambda_c$, where v_r is the slip velocity between two phases, t_* is the particle relaxation time and λ_c the distance traveled between collisions, should be less than 0.1 and depending on the magnitude of flow Reynolds number, boundary conditions for particulate phase have to be modified.

In this paper, scaling factors determining various aspects of particle-fluid interactions and the development of physical models to predict gas-solid turbulent suspension flow fields will be discussed based on two-fluid, continua formulation.

Scaling Rules

The motions of particles in a turbulent flow field are determined by relative density, particle size, inertia, free fall velocity, as well as the correlation between particles and underlying flow turbulence. On the other hand, the particulate phase may influence the turbulence energy spectrum of the gas phase in wave number ranges corresponding to the size of spacing of dispersed-phase dimensions [4]. To investigate the various modes of interaction, the relaxation time t_* of particles has to be compared with various characteristic times of the underlying flow field. t_*, in its simplest definition $\equiv \frac{1}{18} \frac{\rho_s}{\rho} \frac{d_p^2}{\nu}$, is a measure of how quickly a particle of density ρ_s and diameter d_p can respond to changes in the ambient fluid velocity, ν is the kinematic viscosity of the fluid. In the continuum mixture theory, t_* can be redefined based on a particle Reynolds number weighted by the concentration of

solids [5]. If t_* is small compared with a time scale corresponding to some particular flow structure, then the particle will follow the motion of that structure; if not, the particle will tend to be uncoupled from these motion.

Hinze [4] pointed out that the dynamic behavior of a discrete particle will not be determined by the eddies of size much smaller than that of the particles. The effect of these smaller eddies will tend to average out over the particle surface. In the case of turbulent flows, this requires that the particle size be smaller than the important dynamic scales of turbulence before the time scale ratio becomes a useful measure of the particle-fluid interaction.

Let us consider the dynamically smallest eddies in the turbulent flow. These eddies can be characterized by the Kolmogorov microscale η, and the characteristic time scale τ is of order $(\nu/\epsilon)^{1/2}$. The ratio of the particle relaxation time to this time then becomes $\frac{t_*}{\tau} \sim \frac{d_p^2}{\eta^2}\frac{\rho_s}{\rho}$. So for the typical suspension problem we are interested in, i.e., $\rho_s/\rho \geq O(10^2)$, the particles have to be at least one order of magnitude smaller than the Kolmogorov length scale in order to be subjected to the motion of the smallest eddies.

Direct interaction between particles which results from particle-particle collisions can be estimated from the ratio of t_* and the time scale between particle collisions t_c which is given [4] $\sim O(\frac{1}{v_r d_p^2 n})$ for particles of uniform size d_p. v_r is the relative velocity between particles and n is the particle number density. For the case $t_*/t_c \ll 1$, the particle has time to respond to the local velocity field before the next collision so its motion is dominated by the supporting flow forces and the collision which leads to direct interaction between particles can be neglected. Then a solid particle is subjected to a variety of time-varying forces by the ambient fluid flow. For particles with $\rho_s/\rho > 10^2$, the governing forces due to inertia effect (drag) and crossing trajectory effect have been singled out [6,7,8]. To describe the behavior of particles in a turbulent flow, the simplified Basset, Boussinesq and Oseen (BBO) equation has to be solved. This equation in principle cannot be solved unless the relation of the Lagrangian and Eulerian correlations of the random fluid field is known rigorously. However, the particle trajectory can be determined similar to a random walk computation [9] in which a dispersed-phase element is assumed to interact with an typical turbulent eddy as long as the relative displacement of the element with respect to the eddy does not exceed the characteristic eddy size, l_e, and the time of interaction does not exceed the characteristic eddy time, t_e. The selections of l_e and t_e are cleanly arbitrary since turbulent flows composed a spectrum of length scales and time scales.

To gain some insight of the scaling rule for turbulent dispersion, the fundamental dispersion results of Snyder and Lumley [6] are used to compare with the stochastic predictions. The experiments involved the dispersion of individual particles which were isokinetically injected into a grid-generated turbulent flow. The mean flow are uniform in the test region and the detailed turbulent structure were measured downstream of the

injection point. Since the grid-generated turbulent field is homogeneous decaying and is approximately isotropic with fluctuating intensity decreasing in the direction of the mean flow. Typically, grid turbulence is also characterized by self-similar spectral distribution in which a local set of characteristic eddy time scale can be identified. Following Gosman and Ioannides, the eddy time scale is evaluated from the expression $t_e = l_e(\frac{2k}{3})^{-\frac{1}{2}}$ and $l_e = C_\mu^{\frac{3}{4}} k^{\frac{3}{2}}/\epsilon$, where k is the turbulent kinetic energy $(= \frac{1}{2}\overline{u_i' u_i'})$ and ϵ is the isotropic turbulent kinetic energy dissipation rate and $C_\mu = 0.09$. The ratios of t_* over eddy time scales for the three types of mono-dispersed particles used in Snyder and Lumley's experimental setup are plotted on Figure 1. Mean-squared radial dispersion of the particles is plotted as a function of the residence time in the flow for three types of particles.

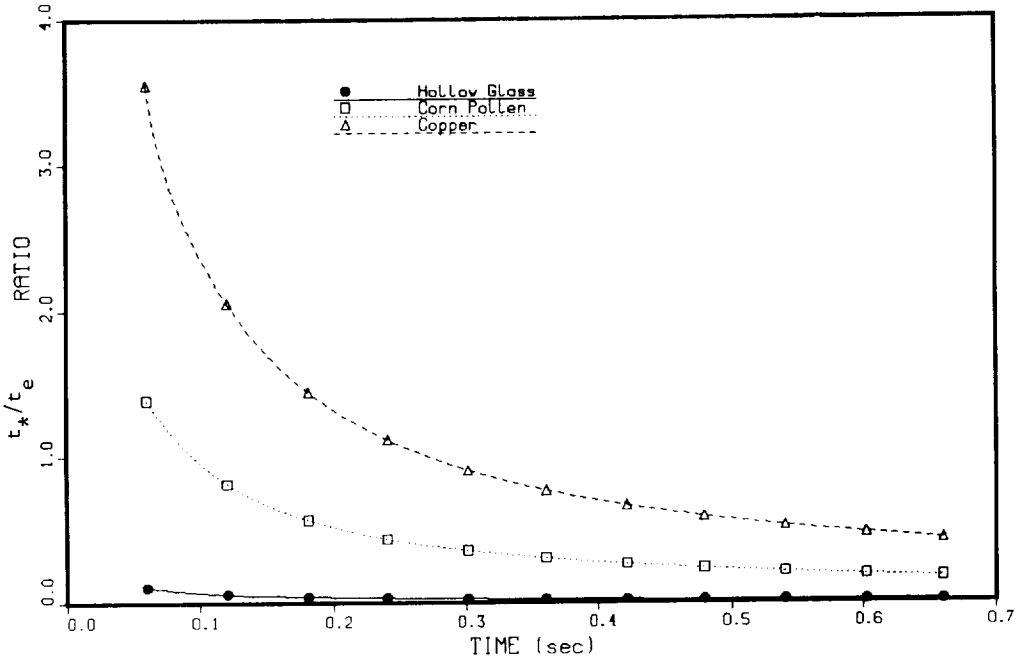

Figure 1. Time scale ratio of various particles in a uniform grid generated turbulent flow

The results are obtained by averaging over 2000 particles following a 4th-order Runge-Kutta integration of the simplified BBO equation (only inertia term retained) using 10 percent of interaction time as integration time step. The agreement between the stochastic model predictions and the measurements for the case of corn pollen (with material density $1000 kg/m^3$ and $87 \mu m$ diameter) are much better compared to the other two cases of hollow glass particles and copper particles. This is not surprising in viewing the scaling rules involved (see Figure 1): the corn pollen particles are most closely associated with the turbulent time scales responsible for dispersion. For light particle such as glass particles, the turbulent eddies responsible for the dispersion should be of higher frequency (smaller time scales), probably Kolmogorov time scales. The net results is that the numerical model underpredicts the dispersion. On the other hand, copper particles should interact

with eddies associated with larger time scales. Using the integral time scale (t_e) results in overpredicting the turbulent dispersion by inertia effects.

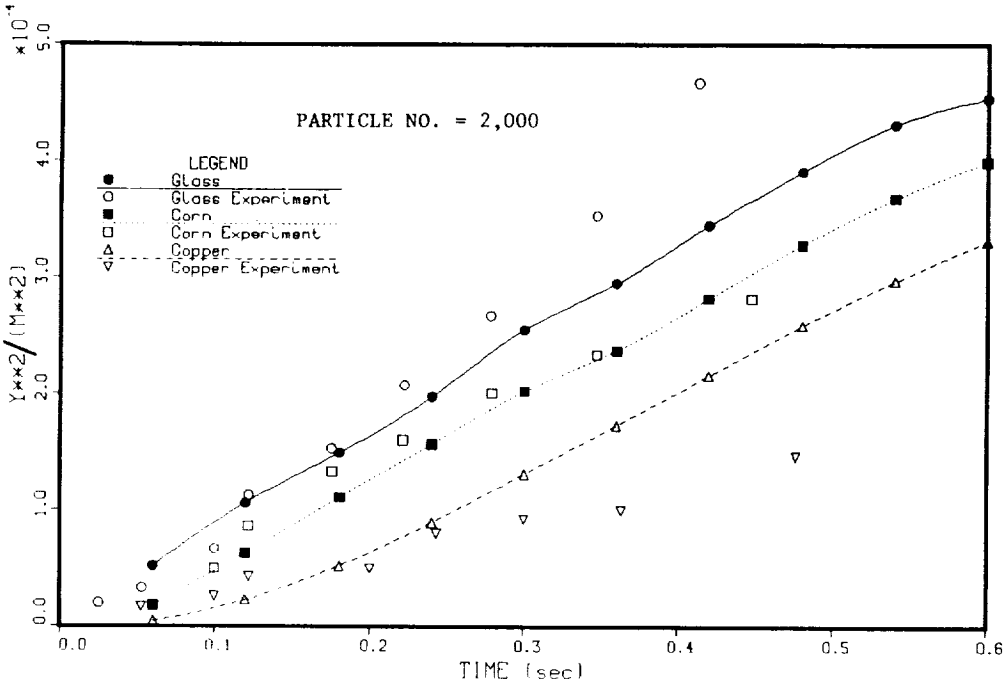

Figure 2. Predicted and Measured particle dispersion in a uniform grid generated turbulent flow

The numerical models used for the calculation in this study do not account for the crossing trajectory effect due to the particle free fall. For the particles studied, especially heavy particles, inertia and crossing trajectories are inseparable at the very downstream of the decay. According to the scaling rule, gravity has an influence on the two-phase flow when $u_t \cong u'$, where u_t is the terminal velocity ($= gt_*$) and u' is the characteristic velocity scale of turbulence. In the grid turbulence $\frac{u'^2}{U_M^2} \propto (\frac{x}{M})^{-1}$, thus we expect the free-fall effects to be insignificant in the decay of the grid turbulence if $\frac{x}{M} \ll O(\frac{U_M}{gt_*})^{1/2}$. Here, U_M is the mean longitudinal velocity along x-axis and M is the mesh size. Only for the smaller particles with $t_* \leq 10$ msec this condition can be satisfied. However, the above calculations indicate the close relationship between the scale parameters and the particle-fluid interactions.

Two-Phase Turbulence Modeling

In most turbulent multiphase flows of practical interest there exists a spectrum of dispersed phase time and length scales. Despite the abundant use of single time and length scale models (such as the $k - \epsilon$ model), the underlying carrying gas turbulence is also dominated by a variety of time scales. A two-phase two-scale turbulence model

based on continuum approach has since been developed [10] according to the scaling rule described above. The modification of particles on the turbulence, the so called modulation effect, has been taken into account for large eddies by mean slip between two phase and small eddies caused by the particle slip velocity on the fluctuation level.

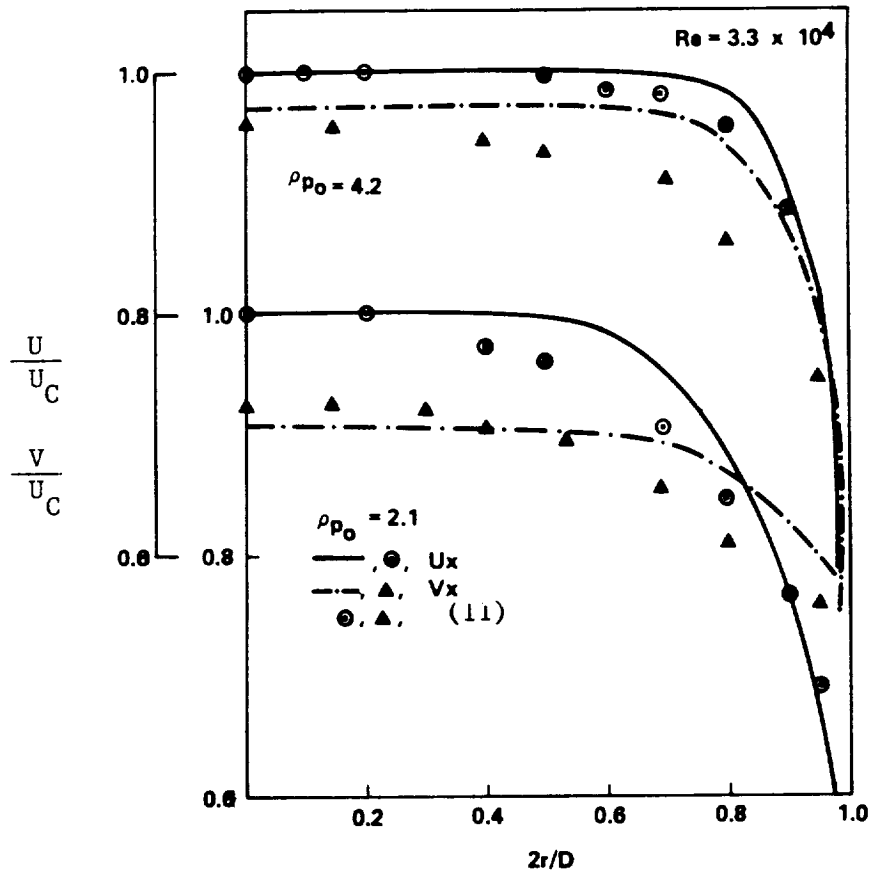

Figure 3. Mean axial velocity profiles across the pipe of gas phase and particulate phase

The turbulent transport equations are summarized here:

$$\frac{\partial}{\partial x_i}(U_i k_p) = \frac{\partial}{\partial x_i}(\frac{\nu_t}{\sigma_{k_p}}\frac{\partial k_p}{\partial x_i}) + P_k - \epsilon_p - \frac{\overline{\rho_p' u_i'}}{\rho t_*}(1 + 0.79\sqrt{Re_p} + 0.013 Re_p)(U_i - V_i) \quad (1)$$

$$\frac{\partial}{\partial x_i}(U_i k_t) = \frac{\partial}{\partial x_i}(\frac{\nu_t}{\sigma_{k_t}}\frac{\partial k_t}{\partial x_i}) + \epsilon_p - \epsilon_t - \frac{2k}{t_*}\frac{\overline{\rho_p}}{\rho}(1 - exp[-\frac{1}{2}\frac{t_*}{\tau}]) \quad (2)$$

$$\frac{\partial}{\partial x_i}(U_i \epsilon_p) = \frac{\partial}{\partial x_i}(\frac{\nu_t}{\sigma_{\epsilon_p}}\frac{\partial \epsilon_p}{\partial x_i}) + \frac{\epsilon_p}{k_p}(C_{p1} P_k - C_{p2}\epsilon_p) \quad (3)$$

$$\frac{\partial}{\partial x_i}(U_i \epsilon_t) = \frac{\partial}{\partial x_i}(\frac{\nu_t}{\sigma_{\epsilon_t}}\frac{\partial \epsilon_t}{\partial x_i}) + \frac{\epsilon_p}{k_p}(C_{t1}\epsilon_p - C_{t2}\epsilon_t) - 2\frac{\overline{\rho_p}}{\rho}\frac{\epsilon_t}{t_*} \quad (4)$$

Here, the k_p and k_t are turbulent kinetic energy of the large-scale energetic eddies and the small-scale transfer eddies and ϵ_p is the energy transfer rate from the large eddies to the transfer eddies. This model composed of two set of scales for gas-phase turbulence. The model is valid for the situation $\tau_p(=\frac{k_p}{\epsilon_p}) \geq t_* \gg \tau$ (Kolmogorov time scale) and particle loading ratio (ρ_p/ρ) of order of 1. This model has been applied to a gas-solid suspension pipe flow by Tsuji et al [11]. In Figure 3, the comparisons are made for two particle loadings with $d_p = 200\mu m$. The predicted velocity profiles are flatter than the experimental data and the relative velocities between two phases decrease with increasing particle loadings. The distance of the sign change of the slip velocity shifts toward the wall for larger particle loadings. The flattening effect by the particles on the fluid velocity distributions can be observed in the Figure 4. Besides this flattening effect, the point of maximum gas phase velocity even deviates from the pipe axis as the loading increases. Such a concave profile indicate counter-diffusion type of momentum transport and cannot be predicted by the current model. It is interesting to note that such profiles were not found in other LDV measurements for similar configuration [12,13], this phenomena should await further experimental confirmation.

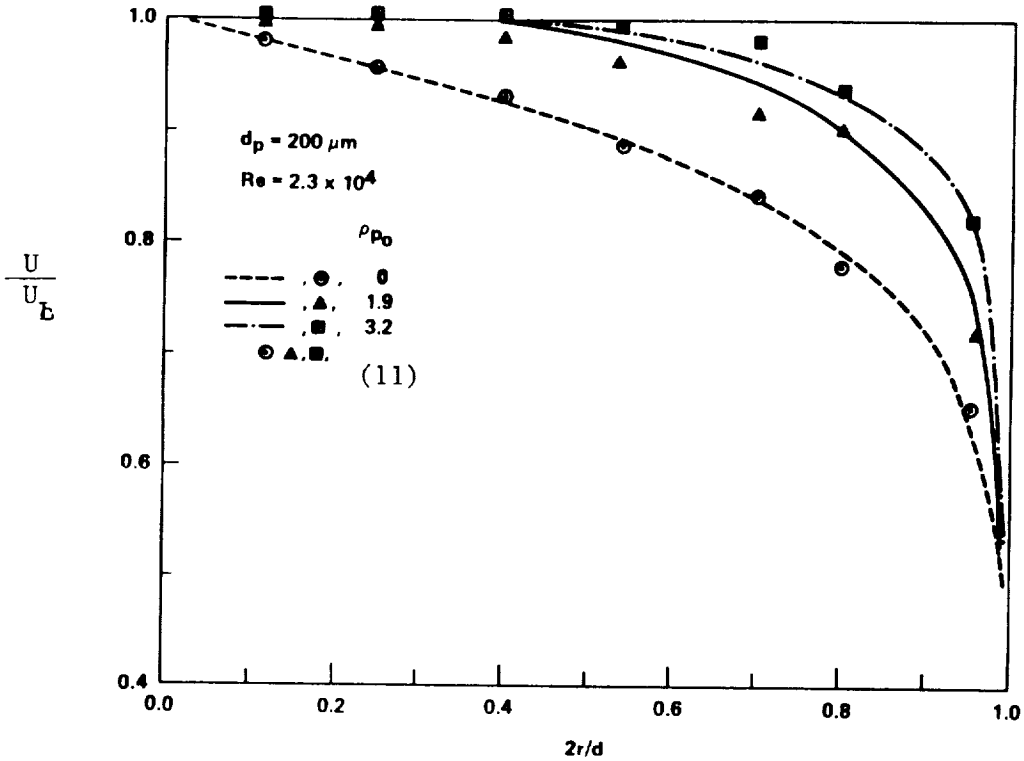

Figure 4. Effect of particle loadings on gas phase velocity profiles

The modulation effect of particles on the turbulence is shown in Figure 5 for longitudinal turbulence intensity profiles for $200\mu m$ particles. Cases with particle size greater than $200\mu m$ were not computed due to model limitation based on the scaling rules. It is

known that fluid turbulence is greatly influenced by the particles and the mode of influence differs with particle size. For larger particles ($\geq 300\mu m$), the turbulence intensities of the fluid are increased due to the presence of particles while suppression of the turbulence properties is observed for smaller particles. It is seen in Figure 5 that for a particle loading of 0.9 the turbulence intensities are reduced by 30 % in the core region. However, the intensity in the core region increases again as the particle loading increases from 0.9 to 3.2 and the intensity in the wall region is monotonously damped. This phenomenon can be explained by the competitive mechanism between modulation due to mean motion and fluctuation motion. The small scale modulation effect always acts as a sink term in the k_t equation while the large eddy motion modulation effect can be extra production or dissipation depending on the signs of $(U_i - V_i)$ and the distribution of mean particle density profiles. The cross-over of the intensity profiles is closely related to the cross-over of mean velocity profiles of gas phase and particulate phase. The relative magnitude of the modulation effects is reasonably well represented by the model.

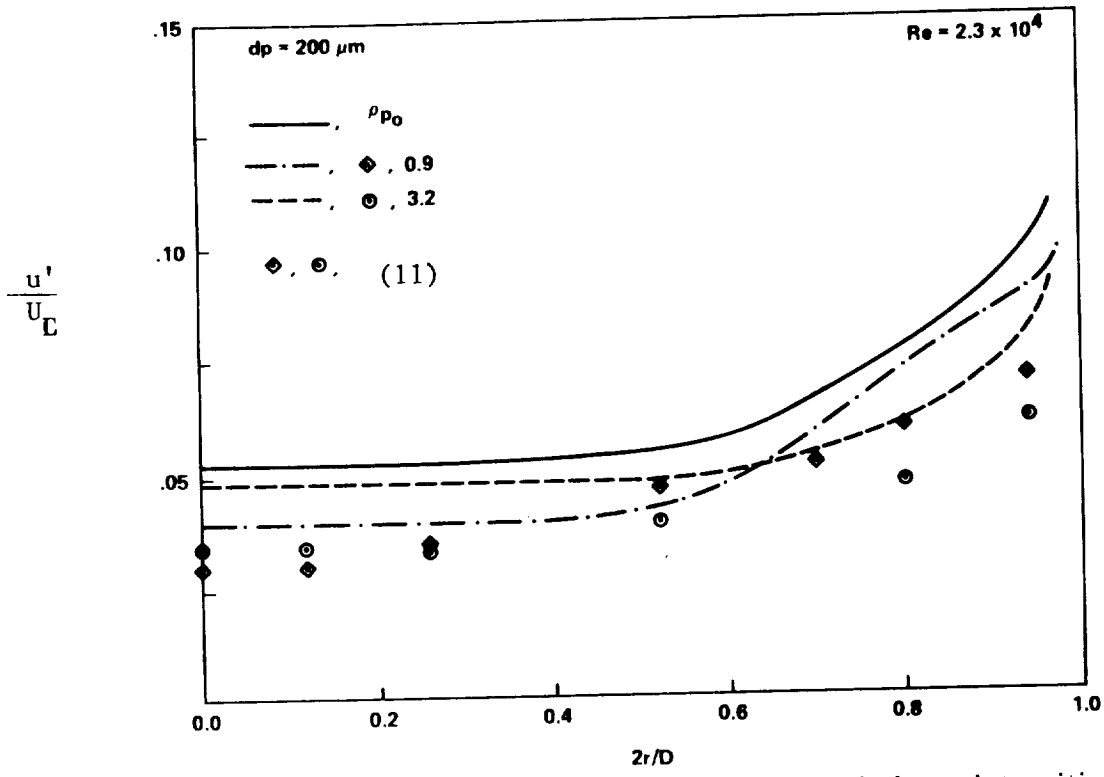

Figure 5. Modulation Of particles on gas phase turbulence intensities

Summary

The modes of particle-fluid is discussed based on the length and time scale ratio, which depends on the properties of the particles and the characteristics of the flow turbulence. For particle size smaller than or comparable with the Kolmogorov length scale and con-

centration low enough for neglecting direct particle-particle interaction, scaling rules can be established in various parameter ranges. The various particle-fluid interaction will give rise to additional mechanisms which will affect the fluid mechanics of the conveying gas phase. These extra mechanisms are incorporated into turbulence modeling method based on the scaling rules. A multiple-scale two-phase turbulence model has been developed, which gives reasonable predictions for dilute suspension flow. Much works is yet to be done to account for the poly-dispersed effects and the extension to dense suspension flows.

Acknowledgements

This work was partially supported by NASA-Marshall Space Flight Center (NAS8-36718).

Reference

1. Lumley, J.L., "Two-Phase and Non-Newtonian Flows," Chapter 7 in Turbulence, ed. P. Bradshaw, Springer-Verlag, 1978.
2. Soo, S. L., Fluid Dynamics of Multiphase System, Blaisdell Pub., 1967.
3. Crowe, C. T., "Two-Fluid versus Trajectory Models," Gas-Solid Flows, ASME FED 35, 91, 1986.
4. Hinze, J. O., Prog. Heat Mass Transfer, 6, 433,1972.
5. Givler, R. C. and Mikatarian, R. R., J. of Fluid Eng. 109, 325, 1987.
6. Snyder, W. H. and Lumley, J. L., J. Fluid Mech. 48, 41, 1971.
7. Calabrese, R. V. and Middleman, S., AIChE. J. 25, 1025, 1979.
8. Wells, M. R. and Stock, D. E., J. Fluid Mech. 136, 31, 1983.
9. Gosman, A. D. and Ioannides, E., AIAA Paper 81-0323, 1981.
10. Chen, C. P., "Numerical Analysis of Confined Recirculating Gas-Solid Turbulent Flows," Gas-Solid Flows, ASME FED 35, 117, 1986.
11. Tsuji, Y. et. al., J. Fluid Mech. 139, 417, 1984. 109, 325, 1987.
12. Steimke, J. L. and Dukler, A. E., Int. J. Multiphase Flows, 9, 751, 1983.
13. Lee, S. L. and Durst, F., Int. J. Multiphase Flows, 8, 125, 1982.